Journal of proteome research

pubs.acs.org/jpr

Article

Human Umbilical Vein Endothelial Cells Survive on the Ischemic TCA Cycle under Lethal Ischemic Conditions

Lisha Mao,[#] Xiaoqi Yuan,[#] Junlei Su,[#] Yaping Ma, Chaofan Li, Hongying Chen, and Fugui Zhang*

Cite This: *J. Proteome Res.* 2022, 21, 2385−2396

Read Online

ACCESS | Metrics & More | Article Recommendations | Supporting Information

ABSTRACT: It is generally believed that vascular endothelial cells (VECs) rely on glycolysis instead of the tricarboxylic acid (TCA) cycle under both normoxic and hypoxic conditions. However, the metabolic pattern of human umbilical vein endothelial cells (HUVECs) under extreme ischemia (hypoxia and nutrient deprivation) needs to be elucidated. We initiated a lethal ischemic model of HUVECs, performed proteomics and bioinformatics, and verified the metabolic pattern shift of HUVECs. Ischemic HUVECs displayed extensive aerobic respiration, including upregulation of the TCA cycle and mitochondrial respiratory chain in mitochondria and downregulation of glycolysis in cytoplasm. The TCA cycle was enhanced while the cell viability was decreased through the citrate synthase pathway when substrates of the TCA cycle (acetate and/or pyruvate) were added and vice versa when inhibitors of the TCA cycle (palmitoyl-CoA and/or avidin) were applied. The inconsistency of the TCA cycle level and cell viability suggested that the extensive TCA cycle can keep cells alive yet generate toxic substances that reduce cell viability. The data revealed that HUVECs depend on "ischemic TCA cycle" instead of glycolysis to keep cells alive under lethal ischemic conditions, but consideration must be given to relieve cell injury.

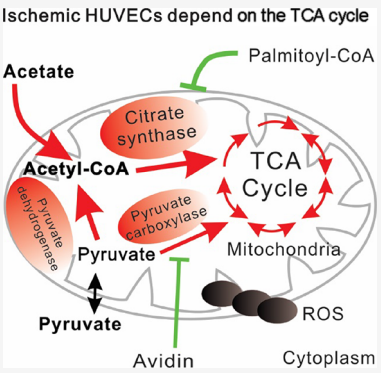

KEYWORDS: *vascular endothelial cells, citrate synthase, tricarboxylic acid cycle, glycolysis, ischemia*

INTRODUCTION

Endothelial cells (ECs) are the orchestral conductors of blood vessel function. The inability of ECs to perform their physiological function (a setting termed EC dysfunction) or pathological blood vessel formation (a process known as pathological angiogenesis)[1] is a common feature of various diseases, such as flap necrosis,[2] limb necrosis, heart failure,[3] stroke, diabetes,[4] and even cancer,[5] affecting millions of people worldwide. Therapeutic intervention to ameliorate EC dysfunction or hamper aberrant angiogenesis could be beneficial in such diseases.[1] Recent studies have proven that EC dysfunction or pathological angiogenesis is accompanied by EC-specific metabolic alterations, thus targeting EC metabolism is emerging as a novel therapeutic strategy.

Cellular metabolism has been well recognized for its role in bioenergetics. In recent years, much light has been shed on the reprogramming cellular metabolism affecting many vital cellular processes, such as cell activation, proliferation, and differentiation;[6] vessel sprouting;[7] and angiogenesis. One of the most notable metabolic reprogrammings is the Warburg effect (a phenomenon known as aerobic glycolysis), which is characterized by a metabolic switch favoring glycolysis over oxidative phosphorylation,[6] under conditions where oxygen is plentiful[8] and sufficient glucose is available.[9]

ECs in the arteries are generally quiescent and exposed to normal/high levels of oxygen and nutrients. Despite their close proximity to oxygenated blood, ECs rely on glycolysis instead of oxidative metabolism for adenosine triphosphate (ATP) production.[7] Specifically, alterations in glucose uptake and utilization, accompanied by a reduction in mitochondrial oxidative phosphorylation, have been demonstrated, mainly due to the activation of pyruvate kinase by the elevated hypoxia-inducible factor (HIF)-1α.[10] The two main fates of the glucose-derived metabolite pyruvate are to be converted to lactate by glycolysis under the regulation of pyruvate kinase and HIF-1α or to be transported to the TCA cycle in the mitochondria.[11] However, it is reported that, under physiological conditions, over 80% of ATP is produced by converting glucose into lactate in ECs, and less than 1% of glucose-derived pyruvate enters the mitochondria for oxidative metabolism through the TCA cycle and subsequent ATP production via the electron transport chain (ETC), which is composed of five multi-subunit complexes.[7] Culic et al. suggested that ATP is generated nearly equivalently by glycolysis and cellular respiration.[12] Glycolysis prevails in ECs, which may be due to its improving EC survival by reducing oxygen consumption and thereby increasing the oxygen availability to perivascular tissues.[13]

Received: April 30, 2022
Published: September 8, 2022

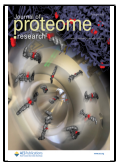

ECs in the venous and lymphatic systems are more likely to encounter hypoxic and nutrient-deprived conditions because of locations and their functions in the vascular tree.[14] Unsurprisingly, under limited oxygen conditions, ECs generally depend on glycolysis to generate energy. Polet and Feron suggested that angiogenic ECs can survive under hypoxic conditions, with high rates of glycolysis and glutaminolysis without coupling to oxidative phosphorylation.[15] Flux analysis demonstrated that glycolysis was the most active process in lymphatic ECs, contributing to more than 70% of the total ATP generation.[16]

It is clear that healthy ECs mainly rely on glycolysis instead of the TCA cycle for survival under normoxic as well as hypoxic conditions. Emerging evidences demonstrated that ECs also survive on glycolysis under pathological conditions, such as pulmonary artery hypertension. Glucose metabolism serving as the primary energy supply generates a more than three-fold glycolytic rate in the pulmonary artery hypertension ECs as compared to normal ECs.[17] Studies in human, avian, rodent, and lamb pulmonary artery hypertension also confirmed this phenomenon.[18] Caruso et al. confirmed the abnormal phenotype of angiogenesis derived from pulmonary artery hypertension patients, associated with enhanced glycolysis and reduced mitochondrial oxidative phosphorylation.[19]

Our study aimed to model tissue engineering scenarios where new vessels would grow or re-connect using highly proliferative human umbilical vein endothelial cells (HUVECs), e.g., transplanted graft. The aim of our study was to investigate how proliferative instead of quiescent cells would survive a period of ischemia (a situation defined as hypoxia plus nutrient deprivation, including deficiency of glucose, amino acids, and fatty acids).[20] This has a great impact of later vessel formation. However, the metabolic phenotype of proliferative ECs under ischemia still needs to be elucidated. We will unveil one novel phenomenon, coined as ischemic TCA cycle, based on the results of high-throughput proteomics, bioinformatics, and kinds of verification.

EXPERIMENTAL SECTION

Cell and Cell Culture

This study was approved by the Stomatological Hospital of Chongqing Medical University Institutional Review Board (No: (2021)058). HUVECs (Otwo Biotech, Shenzhen, China), 1×10^4/mL, 0.2 mL and 1×10^5/mL, 10 mL, were seeded in a 96-well culture plate and a 100 mm dish, respectively. Ischemic conditions were set by culturing cells at the log phase and 60 to 80% confluent with ischemia buffer (1 mM NaH_2PO_4, 24 mM $NaHCO_3$, 2.5 mM $CaCl_2$, 118 mM NaCl, 16 mM KCl, 0.5 mM sodium EDTA, 20 mM sodium lactate, pH 6.8, 37 °C)[21] without glucose and fetal bovine serum (FBS) in a hypoxia incubator ($N_2/O_2/CO_2$, 94%:1%:5%) at 37 °C for up to designated time points. HUVECs after ischemia treatment were incubated in Dulbecco's modified Eagle medium supplemented with 1 g/L glucose and 10% FBS in a regular incubator (5% CO_2, 37 °C) for 24 h to mimic reperfusion conditions.

Apoptosis Analysis

The establishment of a lethal ischemic model of HUVECs and apoptosis analysis was conducted as previously described.[22] This analysis included three groups: a 3 h ischemia group (referred to as group I), a 3 h ischemia/24 h reperfusion group (referred to as group IR), and a 3 h normal control group (referred to as group NC). The exponentially growing HUVECs of these three groups were collected and stained with an Annexin V-FITC/PI assay kit (BestBio, Shanghai, China) following the manufacturer's protocol. Then, cells were subject to flow cytometry analysis using BD influx (BD Biosciences, San Jose, CA, USA). The acquired flow cytometry data were analyzed with FlowJo v10.0 software (Becton, Dickinson and Company, Franklin Lakes, NJ, USA). Each assay condition was done in triplicate.

Proteomics

To identify the respiratory and metabolic status of HUVECs under ischemic conditions, glycolysis and TCA cycle were assessed by proteomics by PTM BIO (PTM Biolabs Co., Ltd., Hangzhou, China) as described.[22] Briefly, HUVECs of I, IR, and NC groups received sonication followed by centrifugation. The supernatant was collected, and the protein concentration was determined with a BCA kit (Beyotime) according to the manufacturer's instructions. Approximately 100 μg of protein of each sample was digested with trypsin for the following experiments. After trypsin digestion, peptides were desalted using a Strata-X C18 SPE column (Phenomenex, Torrance, CA, USA) and vacuum-dried. The peptides were reconstituted in 0.5 M triethylammonium bicarbonate and processed according to the manufacturer's protocol for the 9-plex tandem mass tag (TMT, Thermo Fisher Scientific, MA, USA) kit.[23] The tryptic peptides were fractionated by high-pH reverse-phase high-performance liquid chromatography using an Agilent 300Extend-C18 column (5 μm particles, 4.6 mm ID, 250 mm length). The fractionated peptides were subjected to Q Exactive Plus Hybrid Quadrupole-Orbitrap mass spectrometry (Thermo Fisher Scientific) followed by liquid chromatography−tandem mass spectrometry (LC−MS/MS) in Q Exactive Plus (Thermo Fisher Scientific) coupled online to the UPLC system. Intact peptides were detected in the Orbitrap at a resolution of 70,000. A data-dependent procedure that alternated between one MS scan followed by 20 LC−MS/MS scans with a 15.0 s dynamic exclusion was used. Automatic gain control was used to prevent overfilling of the Orbitrap. Tandem mass spectra were searched against the SwissProt Human database. For the protein quantification method, the LC−MS/MS data were processed using the Mascot search engine (v.2.3.0). The false discovery rate was adjusted to <1%, and the peptide ion score was set at ≥20.

Bioinformatics

To interpret the proteins that were isolated, fractioned, and purified from proteomic detection,[24] Gene Ontology (GO) proteome annotation was performed using the UniProt-GOA database (http://www.ebi.ac.uk/GOA/). For identified proteins that were not annotated by the UniProt-GOA database, InterProScan software was used to assign a GO annotation to the protein based on a protein sequence alignment method. WoLF PSORT (https://wolfpsort.hgc.jp/) was used to predict the subcellular localization of the differentially expressed proteins. In the GO enrichment analysis, proteins were classified by GO annotation into three categories: cellular compartment, biological process, and molecular function. The Kyoto Encyclopedia of Genes and Genomes (KEGG) database was used to identify enriched pathways by the two-tailed Fisher's exact test to compare the enrichment of differentially expressed proteins against all identified proteins. These pathways were classified into hierarchical categories according to the KEGG website (http://www.genome.jp/kegg/). For protein domain enrichment analysis, the InterPro (http://www.ebi.ac.uk/interpro/) database was searched, and the two-tailed Fisher's exact test was employed to compare the enrichment of

https://doi.org/10.1021/acs.jproteome.2c00255
J. Proteome Res. 2022, 21, 2385−2396

differentially expressed proteins against all identified proteins. A corrected *P*-value <0.05 was considered significant. In the functional enrichment-based clustering analysis, quantified proteins in this study were first divided into six quantitative categories according to the quantification P/C ratio: Q1 (0 < I/NC ratio < 1/1.2), Q2 (1/1.2 < I/NC ratio < 1.2), and Q3 (I/NC ratio > 1.2). Then, quantitative category-based clustering was performed. All the substrate categories obtained after enrichment were collated along with their *P*-values and then filtered for those categories that were enriched in at least one of the clusters with a *P*-value <0.05. This filtered *P*-value matrix was transformed using the function $x = -\log 10$ (*P*-value). Finally, these x values were z-transformed for each category. These z-scores were then clustered by one-way hierarchical clustering (Euclidean distance, average linkage clustering) in Genesis. Cluster membership was visualized by a heat map using the "heatmap.2" function from the "gplots" R package (Lucent Technologies, Inc., Murray Hill, NJ, USA). All protein name identifiers were searched against the STRING database (v.10.5, https://stringdb.org/) for protein−protein interactions (PPI). Only interactions between the proteins belonging to the searched data set were selected. STRING defines a metric called the confidence score to define the confidence of the interaction; all interactions that had a confidence score ≥0.7 (medium confidence) were fetched. The interaction network formed in STRING was visualized in Cytoscape (v.3.1, http://www.cytoscape.org/). A graph theoretical clustering algorithm and molecular complex detection (MCODE; https://omictools.com/molecular-complexdetection-tool) were used to analyze densely connected regions.

Western Blot Analysis

Western blot analysis was conducted as previously described.[25] Briefly, HUVECs after the above ischemia/reperfusion treatment were collected, lysed in modified RIPA buffer (Beyotime, Shanghai, China), centrifuged, and quantified using the BCA method (Beyotime) according to the manufacturer's protocol. After quantification of the protein concentration, equal amounts of protein lysate were separated by sodium dodecyl sulfate-polyacrylamide gel electrophoresis according to established protocols. Proteins were transferred from the gels to PVDF membranes (MilliporeSigma, Burlington, MA, USA) in a sandwich model at 200 mA for 90 min. The membranes were then probed with primary antibodies against citrate synthase (1:1000, Zen Bioscience, Sichuan, China), pyruvate carboxylase (1:500, Zen Bioscience), pyruvate dehydrogenase (1:500, Zen Bioscience), lactate dehydrogenase (1:250, Zen Bioscience), pyruvate kinase (1:1000, Zen Bioscience), hypoxia-inducible factor-1 (1:300, Zen Bioscience), or β-actin (1:1000, Zen Bioscience) and incubated at 4 °C overnight. After washing with PBST, all membranes were incubated with HRP-conjugated anti-rabbit/anti-mouse secondary antibodies (1:4000; Abcam, Cambridge, UK) at room temperature for 1 h. The immunoreactive proteins were visualized with a ChemiDoc MP Imaging System (Bio-Rad, Hercules, CA, USA). ImageJ 1.46r (National Institutes of Health, MD, USA) was used to determine the protein expression level, which was recorded as the ratio of the target protein relative to β-actin.

Upregulation or Downregulation of the TCA Cycle

To rescue ischemia-challenged HUVECs, the substrate acetyl-CoA was replenished with acetate solution (Sigma-Aldrich Inc., MO, USA) while pyruvate was supplemented with sodium pyruvate solution (Sigma-Aldrich Inc.), respectively. Briefly, prior to 3 h ischemia treatment, subconfluent HUVECs were treated with acetate solution at concentrations of 0, 5, 10, and 20 mM; sodium pyruvate solution at concentrations of 0, 2.5, 5, and 10 mM; and co-treatment with 20 mM acetate solution and 10 mM sodium pyruvate solution. To test the destiny change of ischemic HUVECs when the TCA cycle was inhibited, the activities of citrate synthase or pyruvate carboxylase were inhibited with palmitoyl coenzyme A lithium salt (palmitoyl CoA, Sigma-Aldrich Inc.) or avidin from egg white (Sigma-Aldrich Inc.), respectively. Briefly, prior to the 3 h ischemia treatment, HUVECs were treated with palmitoyl CoA at concentrations of 0, 50, and 100 μM; with avidin at concentrations of 0, 10, and 20 μg/mL; and with 100 μM palmitoyl CoA and 20 μg/mL avidin.

Cell Viability Assay

Quantitative cell viability was assessed by using Cell Counting Kit-8 (CCK-8; Beyotime) according to the manufacturer's protocol. Briefly, subconfluent HUVECs seeded in 96-well plates were treated with different concentrations of acetate solution and/or sodium pyruvate solution, or palmitoyl CoA and/or avidin under ischemic conditions. The CCK-8 reagent was added to each well, followed by incubation at 37 °C for 60 min and reading absorbance at 450 nm. Each assay condition was done twice.

Activity Tests of PK and CS

More than 10^6/mL centrifuged cells were collected in each sample. HUVECs were washed with PBS and ground using a non-contact ultrasonic cell grinder (Scientz08-III non-contact ultrasonic cell grinder, Ningbo Scientz Biotechnology Co., Ltd., China) with a vibration time of 5 s, an interval of 20 s, power of 3840 W, and a duration of 40 min. Distilled water, standard solutions with different concentrations, and samples of 20 μL were added to control, standard, and test groups, respectively. Vortex mixing and incubation for 30 min after adding 250 μL working solution (The Total Protein Assay Kit using a standard BCA method, Nanjing Jiancheng Bioengineering Institute, China) were performed. A terminating solution of 750 μL was added to each well before detecting the absorbance value at 562 nm. The protein concentration C1 of each sample was calculated. For activity tests of PK (Pyruvate Kinase Assay Kit, Nanjing Jiancheng Bioengineering Institute, China) and CS (Citrate Synthase Assay Kit, Nanjing Jiancheng Bioengineering Institute, China), the initial absorbance A1 was measured at 340 nm for 30 s, then it was accurately bathed in 37 °C for 15 min, and the final absorbance A2 was taken out for 15 min and 30 s. Initial absorbance A1, final absorbance A2, mmol extinction coefficient 6.22 L/(μmol·cm), reaction time 15 min, light path 0.5 cm, total volume of reaction solution 1.195 mL, sampling volume 0.02 mL, and protein concentration of sample C1 gprot/mL were applied to calculate the activity of PK and CS. The calculation formula is

$$\text{kinase activity}\left(\frac{\text{U}}{\text{gprot}}\right) = \frac{\text{A1} - \text{A2}}{6.22 \times 15 \times 0.5} \times \frac{1.195}{0.02 \times \text{C1}}$$

Data Analysis

Student t-test, analysis of variance (Tukey test), and/or nonparametric test (Kruskal−Wallis test) were used to evaluate the differences between groups by SPSS (Version 19.0; IBM Corp., Armonk, NY, USA). $P < 0.05$ was considered statistically significant. The original figures were produced by GraphPad Prism 8 (GraphPad Company, San Diego, CA, USA), and

https://doi.org/10.1021/acs.jproteome.2c00255
J. Proteome Res. 2022, 21, 2385−2396

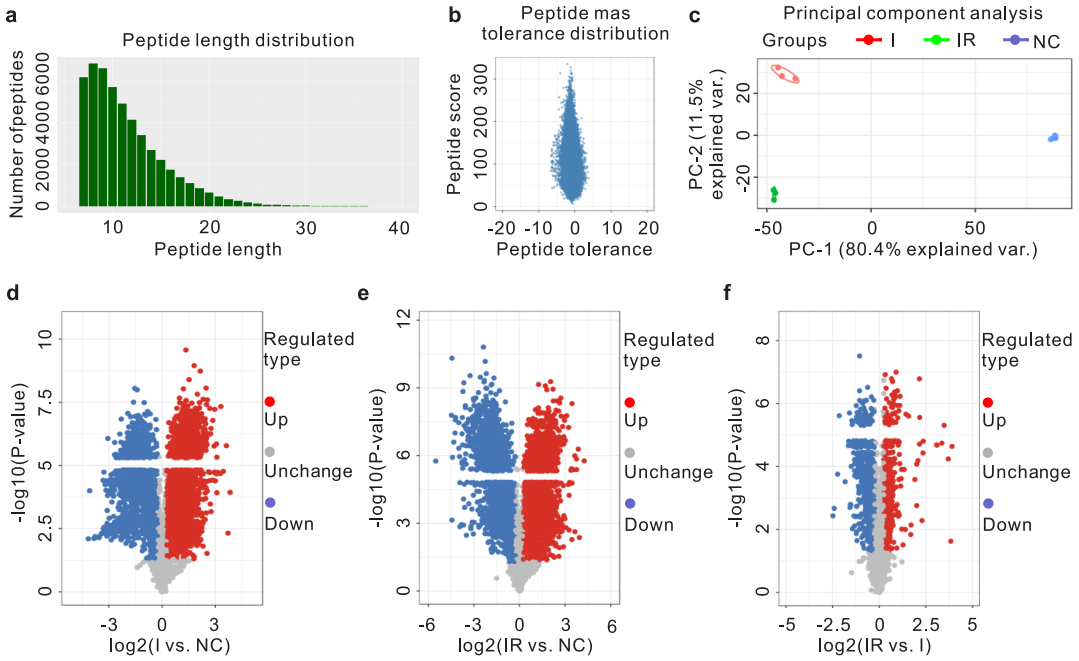

Figure 1. Good biological repeatability and consistency of LC−MS/MS analysis. (A) Most proteins distributed at 7−20 peptides per peptide length distribution. (B) The first-order mass error of all spectra was within 10 ppm by the peptide mass tolerance distribution. (C) Principal component analysis showed extremely good biological repeatability of the protein expression levels. Group NC: 3 h normal control group, group I: 3 h ischemia group, group IR: 3 h ischemia/24 h reperfusion group. (D−F) The differentially expressed proteins had an exceeding degree of consistency between the IR/NC compare group and the I/NC compare group from volcano plots.

figures were assembled by CorelDRAW(R) Graphics Suite X4 (Corel, Ottawa, Ontario, Canada).

RESULTS

Lethal Ischemic Model of HUVECs and Apoptotic Analysis

The optimal lethal ischemia time, 3 h, was verified by Western blotting and confirmed by apoptosis analysis through flow cytometry as previously described.[22] Apoptotic analysis proved that there were statistically significant differences in the apoptotic ratio between experimental groups compared with the control group ($P < 0.05$), but no statistically significant difference between group I and group IR ($P > 0.05$).

Proteomics

The quantitative analysis of the global proteome in HUVECs after the 3 h ischemic and/or 24 h reperfusion treatment or sham treatment was performed by using 9-plex TMT labeling, high-performance liquid chromatography fractionation, and LC−MS/MS analysis. Altogether, a total of 6080 proteins were identified, of which 5401 proteins were quantified (ProteomeXchange Consortium, PXD031313). When quantitatively comparing the ratio between groups (ratios of I/NC, IR/NC, and IR/I), a fold change larger than 1.2 was considered as upregulation, and ratios less than 1/1.2 were regarded as downregulation. A total of 2520 proteins were upregulated and 1856 proteins were downregulated per I/NC ratio ($P < 0.05$, Supplementary Table 1). Most proteins corresponded to 7−20 peptides in terms of number of peptides per protein distribution. The peptide mass tolerance distribution showed that the first-order mass error of all spectra was within 10 ppm. Principal component analysis suggested that protein expression level indicated an extremely good biological repeatability ($n = 3$, respectively). Volcano plots depicted that the differentially expressed proteins in the IR/NC and I/NC groups had an exceeding degree of consistency (Figure 1).

Functional Enrichment

This study mainly focused on the phenotype change of HUVECs after a 3 h lethal ischemia challenge, so the I/NC compare group was set as the target. Functional enrichment was composed of GO enrichment and KEGG pathway enrichment, and the former consisted of enrichments of biological process, cellular component, and molecular function. The biological process enrichment showed that functional upregulation was observed in aerobic respiration, cellular amine metabolic process, cellular respiration, respiratory ETC, etc. Cellular component enrichment illustrated that the inner mitochondrial membrane protein complex, mitochondrial respiratory chain, mitochondrial protein complex, respiratory chain complex, and respiratory chain were enhanced. Molecular function enrichment demonstrated that electron carrier activity, nicotinamide adenine dinucleotide (NADH) dehydrogenase activity, NADH dehydrogenase (ubiquinone) activity, and NADH dehydrogenase (quinone) activities were elevated. KEGG pathway enrichment showed the upregulated pathways including metabolism of glycine, serine, and threonine; TCA cycle; glyoxylate and dicarboxylate metabolism; degradation of valine, leucine, and isoleucine; and tryptophan metabolism (Figure 2).

Functional Enrichment-Based Clustering

Functional enrichment-based clustering was composed of clusterings of the biological process, cellular component, molecular function, and KEGG pathway. The biological process enrichment-based clustering showed that cellular respiration, respiratory ETC, aerobic respiration, mitochondrial transmembrane transport, and regulation of cellular amine metabolic process were upregulated. Cellular component enrichment-based clustering illustrated that mitochondrial respiratory chain,

https://doi.org/10.1021/acs.jproteome.2c00255
J. Proteome Res. 2022, 21, 2385−2396

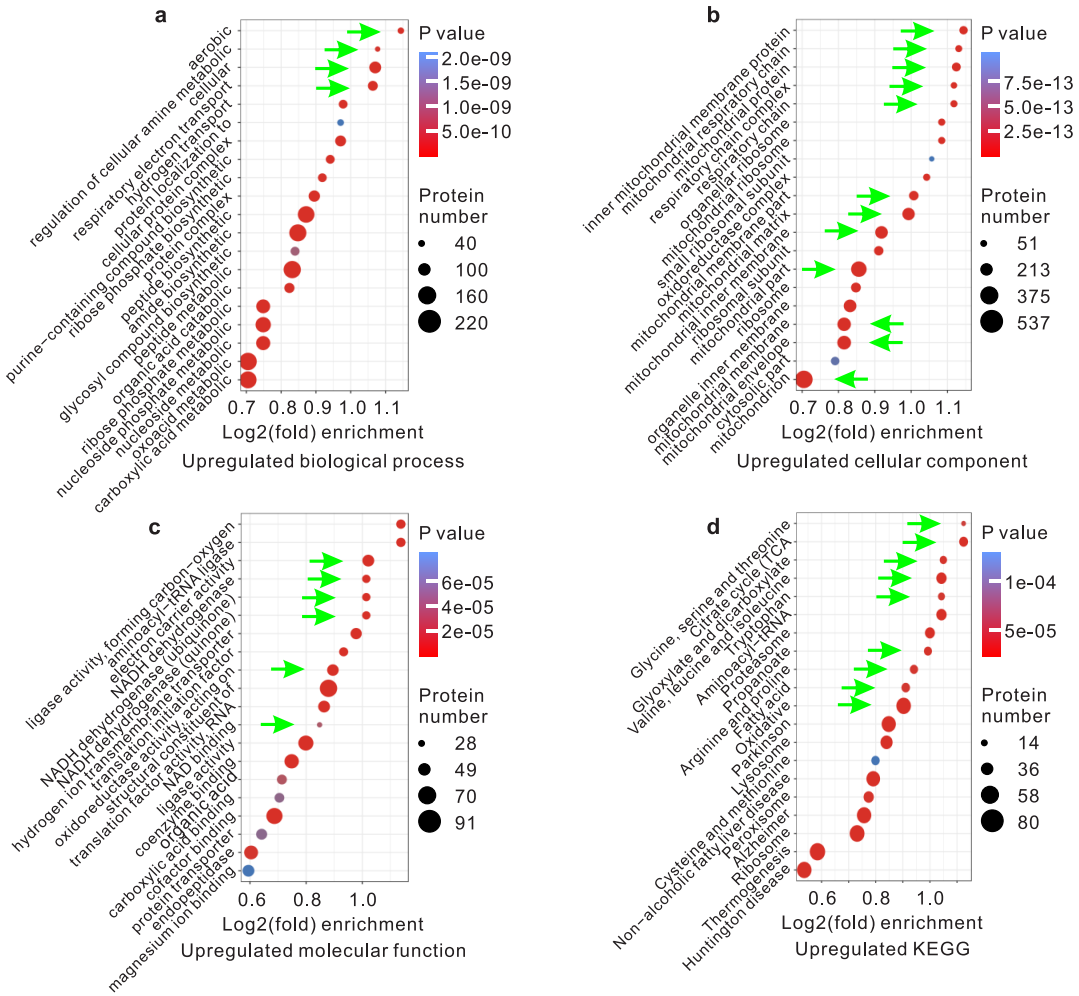

Figure 2. Functional enrichment analysis. (A) The biological process enrichments showed upregulated aerobic respiration, cellular amine metabolic process, cellular respiration, etc. (B) Cellular component enrichment illustrated enhanced inner mitochondrial membrane protein complex and mitochondrial respiratory chain. (C) Molecular function enrichment demonstrated elevated NADH dehydrogenase activity and NADH dehydrogenase (ubiquinone) activity. (D) KEGG pathway enrichment showed the upregulated pathways including metabolism/degradation of amino acids, fatty acid degradation, and TCA cycle. Green arrows point to the elevated aerobic respiration, mitochondrial respiratory chain, NADH dehydrogenase activity, amino acid and fatty acid degradation, and TCA cycle.

respiratory chain, mitochondrial membrane, mitochondrial matrix, mitochondria, and so forth were increased. Molecular function enrichment-based clustering demonstrated that electron carrier activity, NADH dehydrogenase activity, NADH dehydrogenase (ubiquinone) activity, NADH dehydrogenase (quinone) activities, etc., were elevated. KEGG pathway enrichment-based clustering proved the upregulated pathways including metabolism of glycine, serine, and threonine; TCA cycle; pyruvate metabolism; tryptophan metabolism; cysteine and methionine metabolism; degradation of valine, leucine, and isoleucine; and fatty acid degradation (Figure 3).

Western Blot Verification

Proteomics and bioinformatics indicated the downregulation of enzymes regarding glycolysis and upregulation of enzymes regarding the TCA cycle. The results of Western blot analysis were highly consistent with those of LC−MS/MS with upregulated citrate synthase and pyruvate dehydrogenase and decreased pyruvate kinase ($P < 0.01$). Western blot analysis also suggested the quiescence of HIF-1 α (Figure 4). Proteomics and bioinformatics also indicated that β-actin was the most stable and reliable housekeeping protein while the expression levels of other housekeeping proteins, such as GAPDH, α-tubulin, and β-tubulin, varied a lot by proteomics ($P < 0.05$, Supplementary Table 2). Bioinformatics suggested an upregulation trend of most antioxidant protease as well, such as superoxide dismutase, glutathione peroxidase, and glutathione reductase ($P < 0.05$, Supplementary Table 3).

Upregulation or Downregulation of the TCA Cycle

It is interesting to find out that CCK-8 analysis showed that the cell viability of ischemic HUVECs was significantly decreased rather than increased when treated with acetate solution at a concentration of 20 mM ($P < 0.05$), sodium pyruvate solution at concentrations of 5 and 10 mM ($P < 0.05$), and co-treatment with 20 mM acetate and 10 mM pyruvate ($P < 0.01$, Figure 5A). The expression levels of citrate synthase were significantly increased through the solo treatment with 20 mM acetate and co-treatment with 10 mM pyruvate, while the expression level of pyruvate carboxylase was not significantly impacted by Western blot analysis ($P < 0.05$, Figure 5B). It is significantly meaningful to find out that the cell viability of ischemic HUVECs treated with palmitoyl CoA at concentrations of 50 and 100 μM ($P <$ 0.05), with avidin at concentrations of 10 and 20 μg/mL ($P <$

https://doi.org/10.1021/acs.jproteome.2c00255
J. Proteome Res. 2022, 21, 2385−2396

Figure 3. Functional enrichment-based clustering. (A) The biological process enrichment-based clustering showed elevated aerobic respiration, cellular respiration, and cellular amine metabolic process. (B) Cellular component enrichment-based clustering illustrated upregulated mitochondrial respiratory chain, respiratory chain, mitochondrial membrane, mitochondrial matrix, and so forth. (C) Molecular function enrichment-based clustering demonstrated increased NADH dehydrogenase activity, NADH dehydrogenase (ubiquinone) activity, etc. (D) KEGG pathway enrichment-based clustering proved the upregulated pathways including TCA cycle, amino acid metabolism, and fatty acid degradation. Green arrows point to the upregulated aerobic respiration, mitochondrial respiratory chain, NADH dehydrogenase activity, amino acid/fatty acid degradation, and TCA cycle.

0.01), and by co-treatment with 100 μM palmitoyl CoA and 20 μg/mL avidin ($P < 0.01$) was statistically increased (Figure 5C). The expression levels of citrate synthase were slightly decreased through the solo or co-treatment with 100 μM palmitoyl CoA and 20 μg/mL avidin but did not reach significant difference ($P > 0.05$), and the expression levels of pyruvate carboxylase was further downregulated on the basis of ischemia by Western blot analysis (Figure 5D).

https://doi.org/10.1021/acs.jproteome.2c00255
J. Proteome Res. 2022, 21, 2385−2396

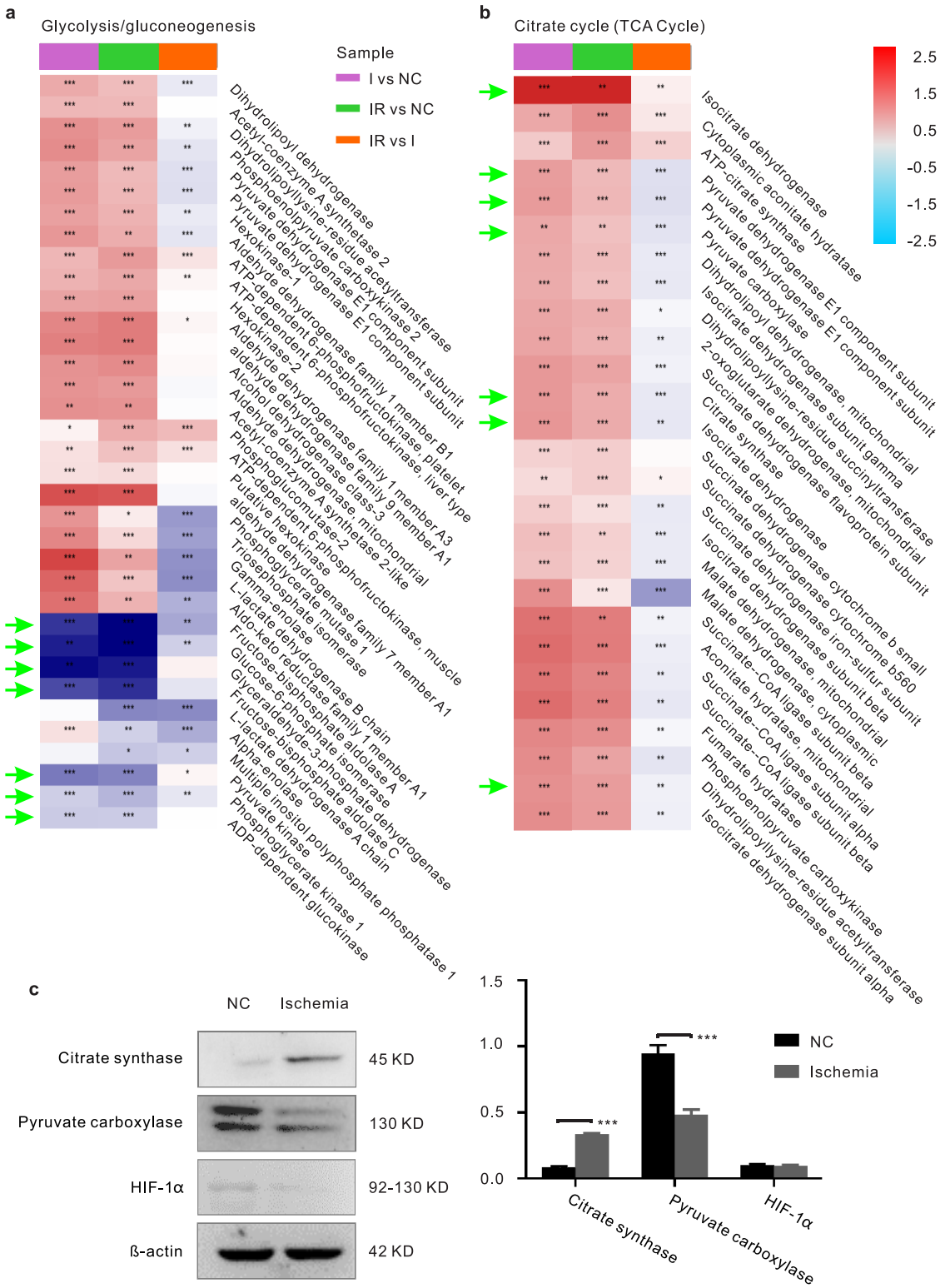

Figure 4. Differentially expressed proteins of glycolysis and TCA cycle between compare groups by bioinformatics and Western blot analysis. (A) Bioinformatics indicated the downregulations of pyruvate kinase, and glucose-6-phosphate isomerase, suggesting the downregulation of glycolysis. (B) Bioinformatics suggested the upregulations of citrate synthase, and pyruvate dehydrogenase, indicating the upregulation of the TCA cycle. (C) Western blot analysis indicated the downregulation of pyruvate kinase, quiescence of HIF-1α, and upregulation of citrate synthase, ***$P < 0.001$. Each assay condition was done in triplicate.

Activity Tests of PK and CS

In order to verify the enzyme activity of PK and CS, a PK assay kit and a CS assay kit were utilized. The PK activity of HUVECs had an upregulated trend after 1 h of ischemia; however, the PK activity declined when HUVECs suffered from 2 h or 3 h ischemia. There was a significant difference in PK activity between the 3 h ischemia group and control group ($P < 0.05$). The CS activity of HUVECs had an upregulated trend as time

https://doi.org/10.1021/acs.jproteome.2c00255
J. Proteome Res. 2022, 21, 2385−2396

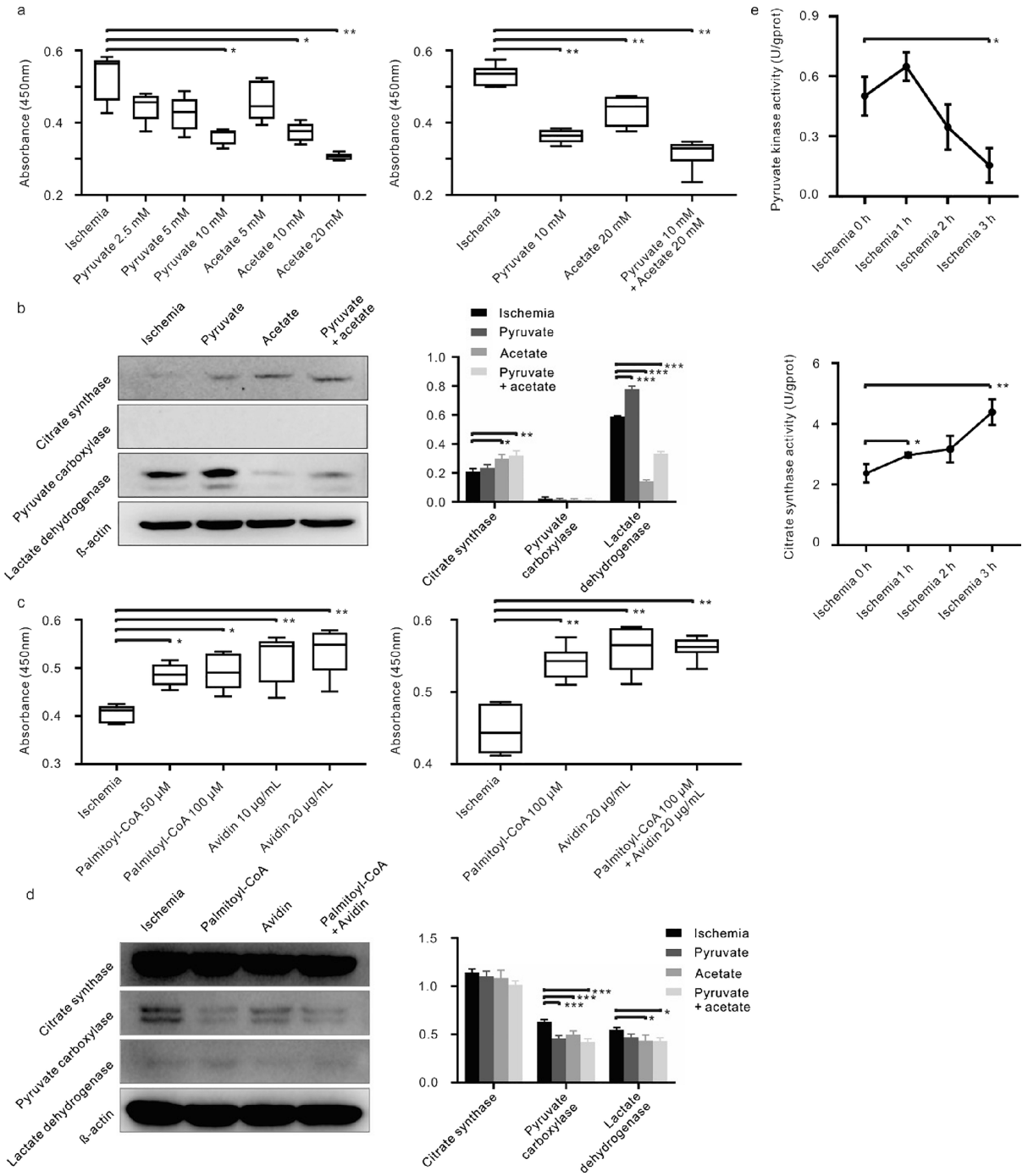

Figure 5. The results of upregulation or downregulation of the TCA cycle of ischemic HUVECs, verified by CCK-8 analysis and Western blot analysis. (A) The cell viability of ischemic HUVECs was significantly decreased when the substrates of the TCA cycle (pyruvate and/or acetate) were added, suggesting a dose-dependent manner. (B) The expression levels of citrate synthase were statistically upregulated when acetate and/or pyruvate were added. (C) The cell viability of ischemic HUVECs was significantly increased when the inhibitor of citrate synthase (palmitoyl CoA) and/or inhibitor of pyruvate carboxylase (avidin) were added. (D) The expression levels of citrate synthase were slightly downregulated but did not reach significant difference, and the level of pyruvate carboxylase was further inhibited after ischemia when palmitoyl CoA and/or avidin were added. (E) The pyruvate kinase activity was first upregulated and then downregulated, and the citrate synthase activity was continuously upregulated. *$P < 0.05$; **$P < 0.015$; ***$P < 0.001$. Each assay condition was done in triplicate.

went by, and there was a significant difference in CS activity between the 3 h ischemia group and control group ($P < 0.01$, Figure 5E).

DISCUSSION

Normal cells adopt glycolysis under a hypoxic/anoxic situation and rely on aerobic respiration under normoxic conditions,[10] but healthy ECs generate most of their energy from glycolysis under both hypoxic and normoxic settings.[26] Our initially established lethal ischemic model of HUVECs suggested that HUVECs depended on the TCA cycle rather than glycolysis for their survival under lethal ischemic conditions. HUVECs were completely disrupted under a microscope after more than 3 h of ischemia and 24 h of reperfusion, which was verified by

https://doi.org/10.1021/acs.jproteome.2c00255
J. Proteome Res. 2022, 21, 2385−2396

uncollected β-actin (a typical housekeeping protein) by Western blot analysis. The apoptosis analysis by flow cytometry also illustrated that there was no statistically significant difference between group I and group IR. These data suggested a successful establishment of the novel lethal ischemic model.

The extremely strong biological repeatability and high degree of consistency by LC−MS/MS analysis also demonstrated the successful setup of the lethal ischemic model. The robust ischemic model was further proven by the extraordinarily same tendency in the I/NC compare group (2520 upregulated proteins and 1856 downregulated proteins) and IR/NC compare group (2538 upregulated proteins and 1882 downregulated proteins) when the fold change was set as >1.2 ($P < 0.05$). The accuracy and credibility of quantitative results increase when a specific protein corresponds to several peptides. Most proteins in this study corresponded to 7−20 peptides regarding the number of peptides per protein distribution, greatly contributing to the reliability of the proteomics data. The peptide mass tolerance distribution showed that the first-order mass error of all spectra was within 10 ppm, which was in line with the high-precision characteristics of the Orbitrap. Principal component analysis showed that the protein expression level obtained extremely excellent biological repeatability in group I, group IR, or group NC ($n = 3$, respectively). The differentially expressed proteins in the IR/NC compare group and I/NC compare group from volcano plots also had a high degree of consistency, which again confirmed the successful establishment of the lethal ischemic model and the high degree of accuracy and consistency of proteomics data.

The biological process enrichments showed that aerobic respiration, cellular amine metabolic process, cellular respiration, and respiratory ETC were upregulated. The biological process enrichment-based clustering also demonstrated that HUVECs prefer aerobic respiration instead of glycolysis under lethal ischemic conditions.

Cellular component enrichment illustrated that the inner mitochondrial membrane protein complex, mitochondrial respiratory chain, mitochondrial protein complex, respiratory chain complex, respiratory chain, etc., were upregulated. Cellular component enrichment-based clustering also verified that it was in the mitochondria where cellular respiration happened. Pettersson-Klein *et al.* suggested that more mitochondria and/or mitochondrial proteins were consistent with increased respiratory capacity.[27] Aerobic respiration consumes oxygen and glucose through oxidative phosphorylation located in the mitochondria.[10] Indeed, mitochondria makes up only 5% of the cellular volume,[28] but mitochondria are the primary oxygen demand in the cell, accounting for roughly 90% of cellular oxygen consumption,[17] 80% of which is coupled to ATP synthesis. ECs had reduced mitochondrial numbers and cellular respiration compared to normal cells, which was consistent with a more than three-fold increase in glycolysis for energy production.[17] However, mitochondria are the sites where pyruvate oxidation, TCA cycle, amino acid metabolism, and fatty acid metabolism happen.[29] This is contrary to glycolysis, which happens in cytoplasm as previously reported but indicates increased aerobic respiration in mitochondria by LC−MS/MS analysis.

Molecular function enrichment demonstrated that electron carrier activity, NADH dehydrogenase activity (used in the ETC for generation of ATP), NADH dehydrogenase (ubiquinone) activity, and NADH dehydrogenase (quinone) activities were elevated. Molecular function enrichment-based clustering also confirmed that HUVECs suffered from a lethal ischemia challenge. These suggested that HUVECs survived through higher NADH dehydrogenase in mitochondria, which could produce more ATP.

KEGG pathway enrichment manifested upregulated pathways including metabolism of glycine, serine, and threonine; TCA cycle; glyoxylate and dicarboxylate metabolism; degradation of valine, leucine, and isoleucine; and tryptophan metabolism. KEGG pathway enrichment-based clustering finally highlighted that the TCA cycle was replenished by amino acid metabolism and fatty acid metabolism under the condition of nutrient deprivation. This was consistent with the fact that glucose and glutamine,[30] as well as fatty acids,[31] are utilized as primary carbon sources for the TCA cycle. Taken together, all the above data suggested that HUVECs utilized amino acid metabolites and fatty acid metabolites to produce ATP in mitochondria through aerobic respiration to promote cell survival.

ECs are addicted to glycolysis according to published papers for two reasons. First, cellular adaptation to hypoxia is mediated by the transcription factor HIF-1α,[32] which was further demonstrated by Huang *et al.*[33] HIF-1α plays a central role in the adaptive regulation of energy metabolism, by triggering a switch from mitochondrial oxidative phosphorylation to anaerobic glycolysis in hypoxic conditions.[34] Ma *et al.* showed that the HIF-1α metabolic effector, pyruvate kinase, is upregulated and is necessary to maintain aerobic glycolysis in infected cells.[35] After glucose is taken inside the cell under the initiation of HIF-1α, it is metabolized from phosphoenolpyruvate to pyruvate under the regulation of pyruvate kinase;[36] finally, pyruvate is metabolized into lactate in the cytoplasm under the regulation of lactate dehydrogenase. HIF-1α also reduces pyruvate dehydrogenase activity leading to the reduced production of acetyl-CoA[37] and decreases the oxidative metabolism of both fatty acids and glucose.[38] Another reason is that glycolysis rapidly generates ATP. Glycolysis can generate similar amounts of ATP as glucose oxidation as long as glucose is not limited in the extracellular milieu.[39] However, oxygen is limited and exogenous glucose and amino acids are deprived in this lethal ischemic model. Therefore, it is quite reasonable to find out that the uninitiated HIF-1α did not lead to the upregulation of pyruvate kinase and downregulation of pyruvate dehydrogenase, which were confirmed by Western blot and enzyme activity analysis.

Metabolic reprogramming requires readily available bioenergetics substrates, such as glucose, amino acids, and fatty acids, to increase mitochondrial respiration.[40] When glucose and glycolysis levels drop, the oxidation of glucose is enhanced, indicating that ECs switch to oxidative metabolism of glucose when glycolysis is impaired (known as the Crabtree effect).[41] However, it is not clear how HUVECs survive from deprived exogenous glucose and amino acids and limited oxygen. We hypothesized that HUVECs will take endogenous amino acids and fatty acids as vital resources to keep themselves alive. Fatty acid oxidation and glutamine metabolism have implicated the function of replenishing the TCA cycle to produce ATP via oxidative phosphorylation.[36,42] HUVECs may also contain numerous small lipid droplets, which are exceptionally rich in mitochondria-like brown adipocytes.[43] Glycolysis produces a net total of only two molecules of ATP per glucose molecule, whereas glucose oxidation yields up to 36 molecules of ATP,[36] or 38 ATP with complete oxidation.[9] The lethal ischemic condition forces mitochondria to make the complete use of any substrate of the TCA cycle, including fatty acids and amino acids

https://doi.org/10.1021/acs.jproteome.2c00255
J. Proteome Res. 2022, 21, 2385−2396

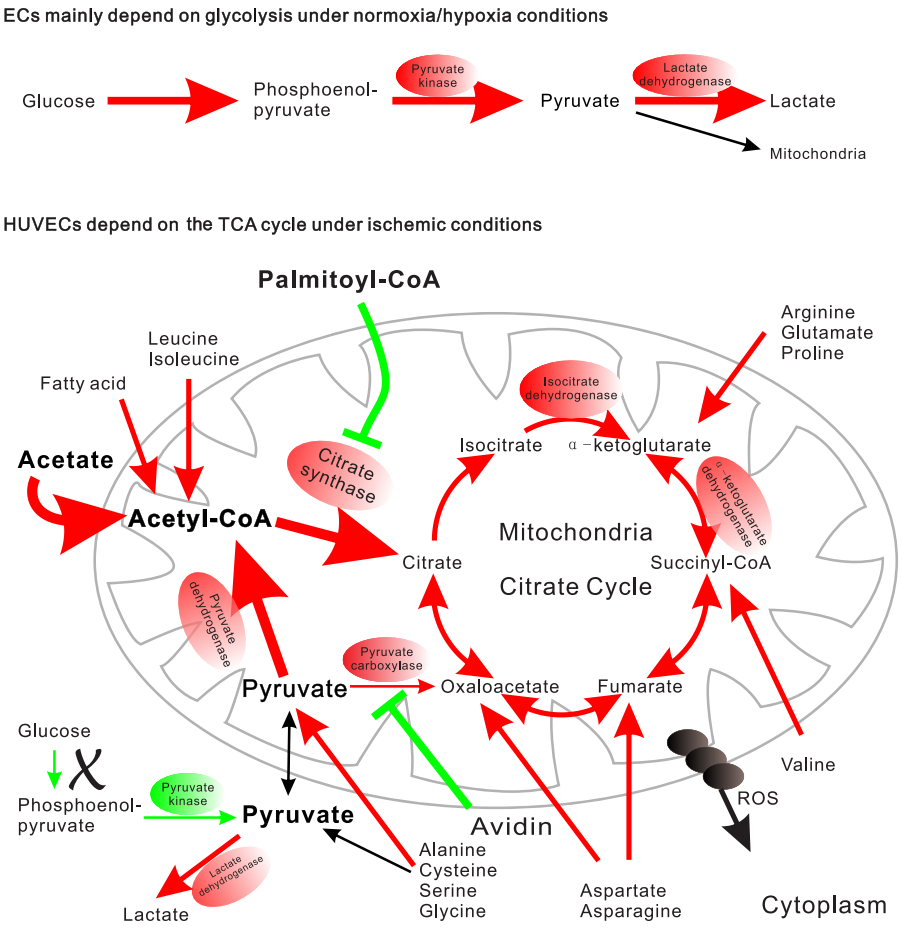

Figure 6. The messtabolic pattern of HUVECs shifts from glycolysis to the TCA cycle through the acetyl-CoA/citrate synthase/citrate pathway to keep cells alive under lethal ischemic conditions.

(such as leucine, isoleucine, alanine, cysteine, serine, glycine, aspartate, asparagine, valine, arginine, glutamate, and proline) in our study, rather than glutamine, which was reported as a major oxidative substrate for coronary ECs.[41] Another reason is that mitochondria in ECs have a high bioenergetic reserve capacity and can increase respiration substantially in stress conditions of glucose deprivation or oxidative stress.[44]

Acetate was recently identified as alternatives to glucose for fueling the TCA cycle in cancer cells, particularly in the condition of hypoxia.[45,46] It is acetyl-CoA synthase that catalyzes acetate-forming acetyl-CoA[45] and citrate synthase that catalyzes acetyl-CoA into citrate, which were upregulated in LC−MS/MS and enzyme activity analysis. The gatekeeper enzyme of the TCA cycle, pyruvate dehydrogenase complex, is responsible for converting pyruvate to acetyl-CoA,[47] and pyruvate carboxylase tetramer is responsible for converting pyruvate into oxaloacetate. We further demonstrated that the protein levels of citrate synthase rather than pyruvate carboxylase were significantly increased by Western blot analysis through the solo treatment with 20 mM acetate and co-treatment with 10 mM pyruvate. It suggested that citrate synthase may dominate the destiny of ischemic HUVECs (Figure 6). The pyruvate carboxylase tetramer may not play a critical role in promoting ischemic HUVEC survival because they were significantly downregulated in the ischemia setting by Western blot analysis. The upregulated pyruvate carboxylase by LC−MS/MS analysis might be due to the dissociation of enzyme tetramers.[48] However, it is interesting to highlight that the cell viability of ischemic HUVECs was significantly decreased by CCK-8 analysis through the solo or co-treatment of acetate and pyruvate. This phenomenon may suggest that the TCA cycle is one indicator of cell injury level in the ischemia setting. A higher level of TCA cycle might be linked with higher release of reactive oxygen substrates, which will destroy the ischemic HUVECs. It is also interesting to find out that this process can be inhibited by the solo or co-treatment of inhibitor of citrate synthase (palmitoyl-CoA) and inhibitor of pyruvate carboxylase (avidin). Thus, it is reasonable to find out an upregulation trend of most antioxidant proteases, such as superoxide dismutase, glutathione peroxidase, and glutathione reductase, in ischemic HUVECs. However, such an upregulated dose could not meet the elimination necessity of more reactive oxygen substrates when the TCA cycle is fueled by pyruvate and acetate.

■ CONCLUSIONS

To sum up, HUVECs depended on the ischemic TCA cycle rather than glycolysis for survival through the enhancement of citrate synthase to produce more ATP in this lethal ischemic model. The TCA cycle in mitochondria was fueled by amino acid metabolism and fatty acid metabolism. This novel phenomenon, coined as the ischemic TCA cycle, shed light on the novel therapeutic strategy to regulate the cells' destiny by promoting VEC survival in free flaps, myocardium, and brain stroke or by preventing VEC survival in anti-angiogenesis therapy of cancers.

https://doi.org/10.1021/acs.jproteome.2c00255
J. Proteome Res. 2022, 21, 2385−2396

■ ASSOCIATED CONTENT

Supporting Information

The Supporting Information is available free of charge at https://pubs.acs.org/doi/10.1021/acs.jproteome.2c00255.

Supplementary Table 1. Differentially expressed protein summary ($P < 0.05$) (PDF)

Supplementary Table 2. Differentially expressed housekeeping protein summary in the I/C compare group. Filtered with the threshold value of expression fold change >1.2 and $P < 0.05$ (PDF)

Supplementary Table 3. Differentially expressed protein summary of the category of antioxidant protease in the I/C compare group. Filtered with the threshold value of expression fold change >1.2 and $P < 0.05$ (PDF)

■ AUTHOR INFORMATION

Corresponding Author

Fugui Zhang − *Department of Oral and Maxillofacial Surgery, Stomatological Hospital of Chongqing Medical University, Chongqing 401147, China;* orcid.org/0000-0002-5298-2160; Phone: +86-23-88860097; Email: 500290@cqmu.edu.cn

Authors

Lisha Mao − *Chongqing Key Laboratory of Oral Diseases and Biomedical Sciences, Chongqing Medical University, Chongqing 401147, China*

Xiaoqi Yuan − *Chongqing Key Laboratory of Oral Diseases and Biomedical Sciences, Chongqing Medical University, Chongqing 401147, China*

Junlei Su − *Chongqing Key Laboratory of Oral Diseases and Biomedical Sciences, Chongqing Medical University, Chongqing 401147, China*

Yaping Ma − *Chongqing Municipal Key Laboratory of Oral Biomedical Engineering of Higher Education, Chongqing 401147, China*

Chaofan Li − *Chongqing Municipal Key Laboratory of Oral Biomedical Engineering of Higher Education, Chongqing 401147, China*

Hongying Chen − *Department of Oral and Maxillofacial Surgery, Stomatological Hospital of Chongqing Medical University, Chongqing 401147, China*

Complete contact information is available at: https://pubs.acs.org/10.1021/acs.jproteome.2c00255

Author Contributions

#L.M., X.Y., and J.S. contributed equally.

Notes

The authors declare no competing financial interest.

The mass spectrometry proteomics data have been deposited to the ProteomeXchange Consortium via the PRIDE [1] partner repository with the dataset identifier PXD031313. The manuscript has data included as electronic supplementary materials.

■ ACKNOWLEDGMENTS

We would like to appreciate Dr. Meredith August at Harvard School of Dental Medicine for her excellent help. This work was supported by the National Natural Science Foundation of China (No. 81400493), Scientific and Technological Research Program of Chongqing Municipal Education Commission (No. KJQN20200429), and Joint Medical Research Project by Chongqing Health Commission and Natural Science Foundation of Chongqing (No. 2020GDRC008).

■ REFERENCES

(1) Goveia, J.; Stapor, P.; Carmeliet, P. Principles of targeting endothelial cell metabolism to treat angiogenesis and endothelial cell dysfunction in disease. *EMBO Mol. Med.* **2014**, *6*, 1105−1120.

(2) Zhang, F. G.; Tang, X. F. New advances in the mesenchymal stem cells therapy against skin flaps necrosis. *World J. Stem Cells* **2014**, *6*, 491−496.

(3) He, X.; Zeng, H.; Chen, S. T.; Roman, R. J.; Aschner, J. L.; Didion, S.; Chen, J. X. Endothelial specific SIRT3 deletion impairs glycolysis and angiogenesis and causes diastolic dysfunction. *J. Mol. Cell. Cardiol.* **2017**, *112*, 104−113.

(4) Kalucka, J.; Bierhansl, L.; Conchinha, N. V.; Missiaen, R.; Elia, I.; Bruning, U.; Scheinok, S.; Treps, L.; Cantelmo, A. R.; Dubois, C.; et al. Quiescent Endothelial Cells Upregulate Fatty Acid beta-Oxidation for Vasculoprotection via Redox Homeostasis. *Cell Metab.* **2018**, *28*, 881−894.e13. e813

(5) Rohrig, F.; Schulze, A. The multifaceted roles of fatty acid synthesis in cancer. *Nat Rev Cancer* **2016**, *16*, 732−749.

(6) Tang, C. Y.; Mauro, C. Similarities in the Metabolic Reprogramming of Immune System and Endothelium. *Front Immunol* **2017**, *8*, 837.

(7) De Bock, K.; Georgiadou, M.; Schoors, S.; Kuchnio, A.; Wong, B. W.; Cantelmo, A. R.; Quaegebeur, A.; Ghesquiere, B.; Cauwenberghs, S.; Eelen, G.; et al. Role of PFKFB3-driven glycolysis in vessel sprouting. *Cell* **2013**, *154*, 651−663.

(8) Gatenby, R. A.; Gillies, R. J. Why do cancers have high aerobic glycolysis? *Nat Rev Cancer* **2004**, *4*, 891−899.

(9) Wang, T.; Marquardt, C.; Foker, J. Aerobic glycolysis during lymphocyte proliferation. *Nature* **1976**, *261*, 702−705.

(10) Palsson-McDermott, E. M.; O'Neill, L. A. The Warburg effect then and now: from cancer to inflammatory diseases. *BioEssays* **2013**, *35*, 965−973.

(11) Serbulea, V.; Upchurch, C. M.; Ahern, K. W.; Bories, G.; Voigt, P.; DeWeese, D. E.; Meher, A. K.; Harris, T. E.; Leitinger, N. Macrophages sensing oxidized DAMPs reprogram their metabolism to support redox homeostasis and inflammation through a TLR2-Syk-ceramide dependent mechanism. *Mol Metab* **2018**, *7*, 23−34.

(12) Culic, O.; Gruwel, M. L.; Schrader, J. Energy turnover of vascular endothelial cells. *Am. J. Physiol. Cell Phys* **1997**, *273*, C205−C213.

(13) Eelen, G.; Cruys, B.; Welti, J.; De Bock, K.; Carmeliet, P. Control of vessel sprouting by genetic and metabolic determinants. *Trends Endocrinol. Metab.* **2013**, *24*, 589−596.

(14) Aird, W. C. Phenotypic heterogeneity of the endothelium: I. Structure, function, and mechanisms. *Circ. Res.* **2007**, *100*, 158−173.

(15) Polet, F.; Feron, O. Endothelial cell metabolism and tumour angiogenesis: glucose and glutamine as essential fuels and lactate as the driving force. *J Intern Med* **2013**, *273*, 156−165.

(16) Yu, P.; Wilhelm, K.; Dubrac, A.; Tung, J. K.; Alves, T. C.; Fang, J. S.; Xie, Y.; Zhu, J.; Chen, Z.; De Smet, F.; et al. FGF-dependent metabolic control of vascular development. *Nature* **2017**, *545*, 224−228.

(17) Xu, W.; Erzurum, S. C. Endothelial cell energy metabolism, proliferation, and apoptosis in pulmonary hypertension. *Compr. Physiol.* **2010**, *1*, 357−372.

(18) Bonnet, S.; Michelakis, E. D.; Porter, C. J.; Andrade-Navarro, M. A.; Thebaud, B.; Haromy, A.; Harry, G.; Moudgil, R.; McMurtry, M. S.; Weir, E. K.; et al. An abnormal mitochondrial-hypoxia inducible factor-1alpha-Kv channel pathway disrupts oxygen sensing and triggers pulmonary arterial hypertension in fawn hooded rats: similarities to human pulmonary arterial hypertension. *Circulation* **2006**, *113*, 2630−2641.

(19) Caruso, P.; Dunmore, B. J.; Schlosser, K.; Schoors, S.; Dos Santos, C.; Perez-Iratxeta, C.; Lavoie, J. R.; Zhang, H.; Long, L.; Flockton, A. R.; et al. Identification of MicroRNA-124 as a Major

Regulator of Enhanced Endothelial Cell Glycolysis in Pulmonary Arterial Hypertension via PTBP1 (Polypyrimidine Tract Binding Protein) and Pyruvate Kinase M2. *Circulation* **2017**, *136*, 2451−2467.
(20) Yapa Abeywardana, M.; Samarasinghe, K. T. G.; Munkanatta Godage, D.; Ahn, Y. H. Identification and Quantification of Glutathionylated Cysteines under Ischemic Stress. *J. Proteome Res.* **2021**, *20*, 4529−4542.
(21) Zhu, T.; Yao, Q.; Wang, W.; Yao, H.; Chao, J. iNOS Induces Vascular Endothelial Cell Migration and Apoptosis Via Autophagy in Ischemia/Reperfusion Injury. *Cell. Physiol. Biochem.* **2016**, *38*, 1575−1588.
(22) Ma, Y.; Li, C.; He, Y.; Fu, T.; Song, L.; Ye, Q.; Zhang, F. Beclin-1/LC3-II dependent macroautophagy was uninfluenced in ischemia challenged vascular endothelial cells. *Genes Dis.* **2022**, *9*, 549−561.
(23) Zhang, X.; Wang, X.; Khurm, M.; Zhan, G.; Zhang, H.; Ito, Y.; Guo, Z. Alterations of Brain Quantitative Proteomics Profiling Revealed the Molecular Mechanisms of Diosgenin against Cerebral Ischemia Reperfusion Effects. *J. Proteome Res.* **2020**, *19*, 1154−1168.
(24) Zhou, Y.; Zhang, D.; Liu, B.; Hu, D.; Shen, L.; Long, C.; Yu, Y.; Lin, T.; Liu, X.; He, D.; Wei, G. Bioinformatic identification of key genes and molecular pathways in the spermatogenic process of cryptorchidism. *Genes Dis.* **2019**, *6*, 431−440.
(25) Zhang, F. G.; Yao, Y.; Feng, Y.; Hua, C. G.; Tang, X. F. Mesenchymal stem cells transduced by stromal cell-derived factor-1alpha augment ischemic free flaps' survival. *Ann. Plast. Surg.* **2011**, *66*, 92−97.
(26) Verdegem, D.; Moens, S.; Stapor, P.; Carmeliet, P. Endothelial cell metabolism: parallels and divergences with cancer cell metabolism. *Cancer Metab.* **2014**, *2*, 19.
(27) Pettersson-Klein, A. T.; Izadi, M.; Ferreira, D. M. S.; Cervenka, I.; Correia, J. C.; Martinez-Redondo, V.; Southern, M.; Cameron, M.; Kamenecka, T.; Agudelo, L. Z.; Porsmyr-Palmertz, M.; Martens, U.; Lundgren, B.; Otrocka, M.; Jenmalm-Jensen, A.; Griffin, P. R.; Ruas, J. L. Small molecule PGC-1α1 protein stabilizers induce adipocyte Ucp1 expression and uncoupled mitochondrial respiration. *Mol Metab* **2018**, *9*, 28−42.
(28) Blouin, A.; Bolender, R. P.; Weibel, E. R. Distribution of organelles and membranes between hepatocytes and nonhepatocytes in the rat liver parenchyma. A stereological study. *J. Cell Biol.* **1977**, *72*, 441−455.
(29) Cortassa, S.; Aon, M. A.; Sollott, S. J. Control and Regulation of Substrate Selection in Cytoplasmic and Mitochondrial Catabolic Networks. A Systems Biology Analysis. *Front Physiol.* **2019**, *10*, 201.
(30) Lunt, S. Y.; Muralidhar, V.; Hosios, A. M.; Israelsen, W. J.; Gui, D. Y.; Newhouse, L.; Ogrodzinski, M.; Hecht, V.; Xu, K.; Acevedo, P. N.; Hollern, D. P.; Bellinger, G.; Dayton, T. L.; Christen, S.; Elia, I.; Dinh, A. T.; Stephanopoulos, G.; Manalis, S. R.; Yaffe, M. B.; Andrechek, E. R.; Fendt, S. M.; Vander Heiden, M. G. Pyruvate kinase isoform expression alters nucleotide synthesis to impact cell proliferation. *Mol. Cell* **2015**, *57*, 95−107.
(31) Schoors, S.; Bruning, U.; Missiaen, R.; Queiroz, K. C.; Borgers, G.; Elia, I.; Zecchin, A.; Cantelmo, A. R.; Christen, S.; Goveia, J.; Heggermont, W.; Goddé, L.; Vinckier, S.; van Veldhoven, P. P.; Eelen, G.; Schoonjans, L.; Gerhardt, H.; Dewerchin, M.; Baes, M.; de Bock, K.; Ghesquière, B.; Lunt, S. Y.; Fendt, S. M.; Carmeliet, P. Fatty acid carbon is essential for dNTP synthesis in endothelial cells. *Nature* **2015**, *520*, 192−197.
(32) Semenza, G. L. Targeting HIF-1 for cancer therapy. *Nat Rev Cancer* **2003**, *3*, 721−732.
(33) Huang, Y.; Lei, L.; Liu, D.; Jovin, I.; Russell, R.; Johnson, R. S.; Di Lorenzo, A.; Giordano, F. J. Normal glucose uptake in the brain and heart requires an endothelial cell-specific HIF-1α-dependent function. *Proc. Natl. Acad. Sci. U. S. A.* **2012**, *109*, 17478−17483.
(34) Goda, N.; Kanai, M. Hypoxia-inducible factors and their roles in energy metabolism. *Int J Hematol* **2012**, *95*, 457−463.
(35) Ma, T.; Patel, H.; Babapoor-Farrokhran, S.; Franklin, R.; Semenza, G. L.; Sodhi, A.; Montaner, S. KSHV induces aerobic glycolysis and angiogenesis through HIF-1-dependent upregulation of pyruvate kinase 2 in Kaposi's sarcoma. *Angiogenesis* **2015**, *18*, 477−488.
(36) De Bock, K.; Georgiadou, M.; Carmeliet, P. Role of endothelial cell metabolism in vessel sprouting. *Cell Metab.* **2013**, *18*, 634−647.
(37) Kim, J. W.; Tchernyshyov, I.; Semenza, G. L.; Dang, C. V. HIF-1-mediated expression of pyruvate dehydrogenase kinase: a metabolic switch required for cellular adaptation to hypoxia. *Cell Metab.* **2006**, *3*, 177−185.
(38) Yang, C.; Jiang, L.; Zhang, H.; Shimoda, L. A.; DeBerardinis, R. J.; Semenza, G. L. Analysis of hypoxia-induced metabolic reprogramming. *Methods Enzymol.* **2014**, *542*, 425−455.
(39) Locasale, J. W.; Cantley, L. C. Metabolic flux and the regulation of mammalian cell growth. *Cell Metab.* **2011**, *14*, 443−451.
(40) Lettieri-Barbato, D. Redox control of non-shivering thermogenesis. *Mol. Metab.* **2019**, *25*, 11−19.
(41) Krutzfeldt, A.; Spahr, R.; Mertens, S.; Siegmund, B.; Piper, H. M. Metabolism of exogenous substrates by coronary endothelial cells in culture. *J. Mol. Cell. Cardiol.* **1990**, *22*, 1393−1404.
(42) Chang, C. H.; Curtis, J. D.; Maggi, L. B., Jr.; Faubert, B.; Villarino, A. V.; O'Sullivan, D.; Huang, S. C.; van der Windt, G. J.; Blagih, J.; Qiu, J.; et al. Posttranscriptional control of T cell effector function by aerobic glycolysis. *Cell* **2013**, *153*, 1239−1251.
(43) Wang, H.; Willershauser, M.; Karlas, A.; Gorpas, D.; Reber, J.; Ntziachristos, V.; Maurer, S.; Fromme, T.; Li, Y.; Klingenspor, M. A dual Ucp1 reporter mouse model for imaging and quantitation of brown and brite fat recruitment. *Mol. Metab.* **2019**, *20*, 14−27.
(44) Dranka, B. P.; Hill, B. G.; Darley-Usmar, V. M. Mitochondrial reserve capacity in endothelial cells: The impact of nitric oxide and reactive oxygen species. *Free Radical Biol. Med.* **2010**, *48*, 905−914.
(45) Corbet, C.; Feron, O. Metabolic and mind shifts: from glucose to glutamine and acetate addictions in cancer. *Curr. Opin. Clin. Nutr. Metab. Care* **2015**, *18*, 346−353.
(46) Zhu, W. W.; Lu, M.; Wang, X. Y.; Zhou, X.; Gao, C.; Qin, L. X. The fuel and engine: The roles of reprogrammed metabolism in metastasis of primary liver cancer. *Genes. Dis.* **2020**, *7*, 299−307.
(47) Golias, T.; Kery, M.; Radenkovic, S.; Papandreou, I. Microenvironmental control of glucose metabolism in tumors by regulation of pyruvate dehydrogenase. *Int. J. Cancer* **2019**, *144*, 674−686.
(48) Rohde, M.; Lim, F.; Wallace, J. C. Pyruvate carboxylase from Saccharomyces cerevisiae. Quaternary structure, effects of allosteric ligands and binding of avidin. *Eur. J. Biochem.* **1986**, *156*, 15−22.

https://doi.org/10.1021/acs.jproteome.2c00255
J. Proteome Res. 2022, 21, 2385−2396